Massive MIMO Two-Way Relaying Systems with SWIPT in IoT Networks

Jinlong Wang, Gang Wang, *Member, IEEE*, Bo Li, *Member, IEEE*, Hongjuan Yang, *Member, IEEE*, Yulin Hu, *Senior Member, IEEE*, and Anke Schmeink, *Senior Member, IEEE*

***Abstract*—In 6th generation (6G) communication networks, ultra-high data rate and reliability are greatly vital for massive user connections and network sensors such as Internet of Things (IoT) devices. Simultaneous Wireless Information and Power Transfer (SWIPT) has been evolved as an efficient strategy to enhance the reliability of wireless communication systems through prolonging the battery lifetime by harvesting energy from the received radio-frequency (RF) signals. Furthermore, cooperative relay sensors in IoT networks can extend the network coverage. In this paper, we consider a massive multiple-input multiple-output (MIMO) two-way relaying system, where the relay node splits the received RF signals into two power streams, one for information decoding (ID) and the other for energy harvesting (EH). Two classical and linear relay precodings, i.e., zero-forcing reception/zero-forcing transmission (ZFR/ZFT) and maximum-ratio combining/maximum-ratio transmission (MRC/MRT), are adopted to satisfy the requirements of high-rate in this relay system. Different from prior work, the SWIPT technique and large-scale fading effects of MIMO channels are taken into account for deriving the asymptotic sum-rates of four prevalent power scaling cases when the number of relay antennas grows to infinity. Finally, the analytical results are evaluated by the presented simulation and numerical results.**

***Index Terms*—Massive MIMO, SWIPT, two-way relaying, ZFR/ZFT, MRC/MRT.**

I. Introduction

DRIVEN by the explosive growth and the massive access of smart devices, ultra-reliable and green communication technologies will be desired in 6th generation (6G) communication networks which provide fast connections and applications [1], [2]. The Internet of Things (IoT) is expected to be as a crucial component of the 6G wireless networks. With the growth of IoT, tens of billions of IoT devices will connect the wireless networks to supply various applications, e.g., industrial communication, e-health care and smart city [3], [4]. It is highly challenging to keep the quality of service (QoS) since the energy of the batteries of IoT devices is limited [5], [6]. Traditional wireless devices in IoT networks with built-in batteries restrict the performance of the communication system due to the operational or economical constraints and the inconvenient changing and replacing of batteries. Simultaneous wireless information and power transfer (SWIPT) has received increasing attention in IoT communication networks, since it has the capability of prolonging the lifetimes of wireless devices [7]. Thus, SWIPT technique has a significant influence on the reliability of wireless communication systems [8]. Furthermore, SWIPT can use the broadcast character of the radio-frequency (RF) signal to enhance the energy efficiency of IoT networks [9], [10]. In [11], two classical and feasible schemes, i.e., time switching (TS) and power splitting (PS) are proposed as SWIPT technique. The TS-based design switches over time between energy harvesting (EH) and information decoding (ID) processing [12], while the PS-based one splits the received RF signals into two power streams, one for ID and the other for EH [13].

A. Related works

To further improve the communication performance, one other crucial technique, massive multiple-input multiple-output (MIMO), has been adopted into the relay systems [14]–[17]. It has been shown that MIMO relay system can not only improve the rate performance but also extend the network coverage of wireless communication system when compared with the single-antenna device-to-device system [18], [19]. Specifically, the multi-pair massive MIMO two-way relay system where full-duplex (FD) mode was applied was considered in [20], the asymptotic spectral efficiencies with two typical beamformings at a relay, i.e., zero reception/zero-forcing transmission (ZFR/ZFT) and maximum-ratio combining/maximum-ratio transmission (MRC/MRT), were derived and analyzed. Although the massive MIMO relay system has a considerable rate in [20], that the source nodes are equipped with only one single antenna limits the system performance. Similarly, in [21], [22], the sum-rates of four power scaling cases in the same system with antenna correlation was investigated to improve the spectral efficiencies of relay system. However, the impact of path loss is not yet understood. This theoretical performance analysis is much more significant for the practical application of massive MIMO relay system.

Besides, MIMO communication systems can dramatically harvest more energy from the received RF signals [23]–[25]. Additionally, by equipping multiple antennas at the transmitter, RF energy can be more effectively transferred to the receiver compared with the device installing a single antenna. Hence, MIMO relay systems with SWIPT technique have been widely investigated [26]–[32]. In particular, a MIMO relaying system which adopts the TS protocol was considered in [26], where the rate was maximized by designing the robust beamforming matrices of transceivers under energy constraints. In [27], the TS scheme was adopted for massive MIMO relay systems,

Manuscript received XXXX, 2020; revised XXXX, 2020. This work was supported in part by the National Natural Science Funding of China under Grant 61671184 and Grant 61901137. *(Corresponding author: Bo Li.)*

J. Wang, G. Wang, B. Li and H. Yang are with the Communication Research Center, Harbin Institute of Technology, Harbin 150001, China (e-mail: wjl200609@gmail.com; gwang51@hit.edu.cn; libo1983@hit.edu.cn; hjyang@hit.edu.cn).

Y. Hu and A. Schmeink are with the ISEK Research Group, RWTH Aachen University, D-52074 Aachen, Germany (e-mail: hu@isek.rwth-aachen.de; schmeink@isek.rwth-aachen.de).

and it has indicated that the achievable rate would approach to the deterministic expression as the amount of relay antennas increases. A multi-antenna relay communication system which contain multiple users has been studied in terms of TS powered relay nodes in [28]. A robust precoding scheme which maximizes the sum-rate of the multi-user relay system has been proposed by the author of [28]. Additionally, in [32], a design of the PS factor and the beamforming matrices at the transceivers for a MIMO two-way relay system based on maximizing the energy efficiency was introduced, where one source is capable of SWIPT. However, massive MIMO two-way relaying systems where the relay is capable of PS has not been investigated so far.

B. Motivation

To achieve the considerable and reliable communication, a feasible way is adopting SWIPT and MIMO techniques into the relay system. It is noteworthy that MIMO technique can increase the energy efficiency and spectral efficiency. On the one hand, SWIPT technique can extend the life time of communication devices. On the other hand, the relay node can be used to expand the coverage of the communication network.

Although these related works mentioned above have established a solid foundation for the relay system with SWIPT, there are still many intractable issues needed to be solved. In particular, the authors in [12], [13], [30] studied a two-way relay system with SWIPT. The rate performance is far from the ideal results due to the users equipped with a single antenna. Besides, the authors in [27] focused on the performance analysis of massive MIMO two way relay with EH, while they ignored the large-scale fading of MIMO channel when deriving the expression of the deterministic rate. Accordingly, the performance of two-way relay system with SWIPT is still far from being well addressed.

Inspired by the above description, in this paper, we investigate the massive MIMO two-way relay system, where SWIPT is used at the relay, and derive the asymptotic sum-rate of the system. Different from the existing relaying system, PS-based relay node and large-scale fading are introduced. Moreover, massive antennas make the performance analysis much challenging. Based on the derivation of the asymptotic sum-rate, the impacts of various parameters, e.g,, PS factor and placement ratio, upon the rate performance are analyzed.

C. Contributions

In this paper, we consider a massive MIMO two-way relaying system with a PS relay node. The main contributions are fourfold:

- We propose a massive MIMO two-way relaying system where the relay is capable of PS. The system model distinguishes from the existing relaying system, since the SWIPT technique and large-scale fading effects of MIMO channels are considered.
- Two classical and linear relay precodings, i.e., ZFR/ZFT and MRC/MRT, are adopted to satisfy the requirements of high-rate in this relay system. The deterministic sum-rate with two precodings are derived when the number of relay antennas increases to infinity.
- After obtaining the deterministic sum-rates, the corresponding asymptotic performance of four classical power scaling cases has been studied and analyzed.
- Simulations are conducted to evaluate the asymptotic performance of the achievable sum-rates. Besides, the PS factor, placement ratio and antenna numbers of users have been investigated to improve the sum-rates of the relaying system.

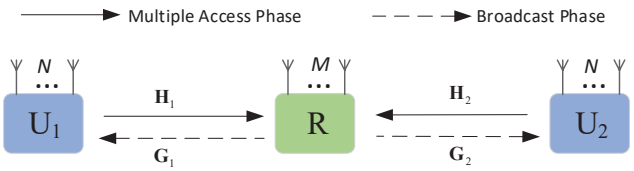

(a) Massive MIMO two-way relaying system.

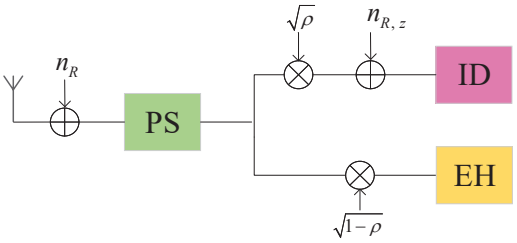

(b) PS scheme at the relay node.

Fig. 1: Massive MIMO two-way relaying system with a PS relay node.

The rest of the paper is outlined as follows. In Section 2, the massive MIMO two-way relaying system with SWIPT is introduced in detail. The deterministic sum-rate with two classical and linear precodings are derived in Section 3. Section 4 provides the asymptotic sum rate of four prevalent power scaling cases. In Section 5, numerical results are conducted to verify the analytical results. Finally, Section 6 gives the conclusion.

II. System Model

We consider a massive MIMO two-way relaying system as illustrated in Fig. 1, where one PS relay R helps two users to communicate, denoted as U_1 and U_2. Each user has a small number of antennas N, while R is employed with a large number of antennas M, i.e., $M \gg N$. According to [33]–[35], we assume that all the channel characteristics vary with time slowly enough so that they can be perfectly estimated by utilizing the feedback channels or the training sequences. Moreover, the amplify-and-forward mode is applied. Two users have their steady power supplies, while the transmission power of R relies on the RF energy sent from two users. The SWIPT technique is adopted at R, and the PS scheme is considered. Furthermore, R utilizes the stored energy to broadcast the ID signal to users.

With the half-duplex relay mode, the communication period block T is equally partitioned into two separate phases, i.e.,

a multiple access (MAC) phase and a broadcast (BC) phase. In the MAC phase, two users transmit their signals to R. The received signal at R can be written as

$$\mathbf{y}_R = \sqrt{\frac{P_U}{N}}\mathbf{H}_1\mathbf{x}_1 + \sqrt{\frac{P_U}{N}}\mathbf{H}_2\mathbf{x}_2 + \mathbf{n}_R, \quad (1)$$

where $\mathbf{x}_i \in \mathbb{C}^{N\times 1}$ denotes the symbol vector at U_i with $\mathbb{E}\left[\mathbf{x}_i\mathbf{x}_i{}^H\right] = \mathbf{I}_N$, $(\cdot)^H$ is the conjugate transpose operation of one matrix, $\mathbf{H}_i \in \mathbb{C}^{M\times N}$ is the MIMO channel matrices of U_i-to-R link. Moreover, following [26], [30], $\mathbf{H}_i$ can be denoted as $\mathbf{H}_i = \sqrt{L_i}\breve{\mathbf{H}}_i$, where L_i stands for the large-scale fading, $\breve{\mathbf{H}}_i$ indicates the small-scale fading with variance $\varphi_{u_i r}^2$. $\mathbf{n}_R$ represents the zero-mean additive white Gaussian noise (AWGN) vector at R with covariance matrix $\sigma_R^2\mathbf{I}_M$. Note that the average power allocation beamforming scheme, i.e., $\mathbf{F}_i = \sqrt{P_U/N}\mathbf{I}_N$, is adopted at U_i and P_U is the transmission power of two users.

The received RF signal at R is split into two portions with the PS factor $\rho \in (0,1)$, and ρ portion is used for ID, $1-\rho$ portion is for EH. Assuming that PS factors in terms of all antennas of the relay are identical for the purpose of reducing the complexity of massive MIMO relay system. According to [11], the ID signal at R is represented by

$$\mathbf{y}_{R,ID} = \sqrt{\rho}\left(\sqrt{\frac{P_U}{N}}\left(\mathbf{H}_1\mathbf{x}_1 + \mathbf{H}_2\mathbf{x}_2\right) + \mathbf{n}_R\right) + \mathbf{n}_{R,\,z}, \quad (2)$$

where $\mathbf{n}_{R,\,z}$ is PS signal processing noise at R with covariance matrix $\sigma_{R,\,z}^2\mathbf{I}_M$. The harvested energy at R is given by[1] [11], [30]

$$E_H = \frac{T}{2}\eta\left(1-\rho\right)\mathrm{tr}\left(\frac{P_U}{N}\sum\nolimits_{i=1}^{2}\mathbf{H}_i\mathbf{H}_i^H\right), \quad (3)$$

where $\mathrm{tr}\left(\cdot\right)$ indicates the trace operation of one matrix and $\eta \in (0,1]$ denotes the energy conversion efficiency of R. In addition, we define the power factor of R as $E_R \triangleq E_H\Big/(T/2) = \eta\left(1-\rho\right)\mathrm{tr}\left(\frac{P_U}{N}\sum_{i=1}^{2}\mathbf{H}_i\mathbf{H}_i^H\right)$.

In the BC phase, R utilizes the harvested energy to transmit the ID signal with a precoding matrix $\mathbf{F}_R \in \mathbb{C}^{M\times M}$ as $\mathbf{x}_R = \mathbf{F}_R\mathbf{y}_{R,ID}$ to two users. The received signal at U_i is

$$\mathbf{y}_i = \mathbf{G}_i\mathbf{F}_R\sqrt{\rho}\sqrt{\frac{P_U}{N}}\left(\mathbf{H}_{\bar{i}}\mathbf{x}_{\bar{i}} + \mathbf{H}_i\mathbf{x}_i\right) + \mathbf{G}_i\mathbf{F}_R\sqrt{\rho}\mathbf{n}_R + \mathbf{G}_i\mathbf{F}_R\mathbf{n}_{R,\,z} + \mathbf{n}_i, \quad (4)$$

where $\bar{i}$ is used to denote the desired signal of the paired user, e.g., $\bar{i} = 1$ for $i = 2$ and $\bar{i} = 2$ for $i = 1$. $\mathbf{G}_i \in \mathbb{C}^{N\times M}$ is the MIMO channel matrix of R-to-U_i link. Similar to $\mathbf{H}_i$, $\mathbf{G}_i$ is modeled as $\mathbf{G}_i = \sqrt{L_i}\breve{\mathbf{G}}_i$, and $\breve{\mathbf{G}}_i$ indicates the small-scale fading with variance $\varphi_{ru_i}^2$. $\mathbf{n}_i$ is the AWGN at U_i with covariance matrix $\sigma_i^2\mathbf{I}_N$. As stated in [20], [21], the self-interference term $\mathbf{G}_i\mathbf{F}_R\sqrt{\rho}\sqrt{\frac{P_U}{N}}\mathbf{H}_i\mathbf{x}_i$ can be integrally cancelled. Therefore, the received signal at U_i is obtained as

$$\mathbf{y}_i = \sqrt{\frac{P_U}{N}}\sqrt{\rho}\mathbf{G}_i\mathbf{F}_R\mathbf{H}_{\bar{i}}\mathbf{x}_{\bar{i}} + \sqrt{\rho}\mathbf{G}_i\mathbf{F}_R\mathbf{n}_R + \mathbf{G}_i\mathbf{F}_R\mathbf{n}_{R,\,z} + \mathbf{n}_i. \quad (5)$$

[1]Compared to EH signals, the noise power is negligible. Therefore, in this paper, the effect of the noise term is ignored for EH.

According to (5), the instantaneous achievable rate at U_i is given by

$$R_i = \frac{1}{2}\log_2\det\left(\mathbf{I}_N + \left(\frac{P_U}{N}\rho\mathbf{Q}_i\right)\times\left(\left(\rho\sigma_R^2 + \sigma_{R,\,z}^2\right)\mathbf{W}_i + \sigma_i^2\mathbf{I}_N\right)^{-1}\right), \quad (6)$$

where $\mathbf{Q}_i = \left(\mathbf{G}_i\mathbf{F}_R\mathbf{H}_{\bar{i}}\right)\left(\mathbf{G}_i\mathbf{F}_R\mathbf{H}_{\bar{i}}\right)^H$ and $\mathbf{W}_i = \mathbf{G}_i\mathbf{F}_R\mathbf{F}_R^H\mathbf{G}_i^H$. Based on (6), the instantaneous achievable sum-rate of massive MIMO two-way relaying system is represented by

$$R_{sum} = \sum\nolimits_{i=1}^{2} R_i. \quad (7)$$

III. Deterministic sum-rates with ZFR/ZFT and MRC/MRT relay precoding

According to [21] and [22], the instantaneous achievable rate will approach a deterministic rate when the number of relay antennas becomes large. To study the asymptotic performance of massive MIMO relay systems, the deterministic sum-rates with two linear and classical precodings are introduced in this section.

A. Deterministic sum-rate with ZFR/ZFT relay precoding

1) ZFR/ZFT processing at the relay: With ZFR/ZFT precoding, the relay employs the ZFR technique to deal with the received signals, and applies the ZFT technique to forward the processed signals. The ZFR/ZFT relay precoding matrix is written as $\mathbf{F}_{zf} = \beta_{zf}\bar{\mathbf{F}}_{zf}$. β_{zf} is the amplification factor of ZFR/ZFT relay precoding and $\bar{\mathbf{F}}_R$ is shown as

$$\bar{\mathbf{F}}_{zf} = \mathbf{G}_{BC}^H\left(\mathbf{G}_{BC}\mathbf{G}_{BC}^H\right)^{-1}\mathbf{T}\left(\mathbf{H}_{MAC}^H\mathbf{H}_{MAC}\right)^{-1}\mathbf{H}_{MAC}^H, \quad (8)$$

where $\mathbf{G}_{BC} = \begin{pmatrix}\mathbf{G}_1^T & \mathbf{G}_2^T\end{pmatrix}^T$, $\mathbf{H}_{MAC} = \begin{pmatrix}\mathbf{H}_1 & \mathbf{H}_2\end{pmatrix}$ and $\mathbf{T} = \begin{pmatrix}\mathbf{0}_{N\times N} & \mathbf{T}_1\\ \mathbf{T}_2 & \mathbf{0}_{N\times N}\end{pmatrix}$ denotes a block permutation matrix which is used to align transmission information of two users. Under the power constraint at R, i.e., $\mathrm{tr}\left[\mathbb{E}\left(\mathbf{x}_R\mathbf{x}_R^H\right)\right] = P_R$, we obtain

$$\beta_{zf}{}^2\left(\frac{P_U}{N}\rho\mathrm{tr}\left(\bar{\mathbf{F}}_{zf}\mathbf{H}_{MAC}\mathbf{H}_{MAC}^H\bar{\mathbf{F}}_{zf}^H\right) + \rho\sigma_R^2\mathrm{tr}\left(\bar{\mathbf{F}}_{zf}\bar{\mathbf{F}}_{zf}^H\right) + \sigma_{R,\,z}^2\mathrm{tr}\left(\bar{\mathbf{F}}_{zf}\bar{\mathbf{F}}_{zf}^H\right)\right) = P_R. \quad (9)$$

Therefore, the amplification factor of ZFR/ZFT relay precoding can be written as (10) at the top of next page.

2) Deterministic sum-rate with ZFR/ZFT relay precoding: As shown in (6), the sum-rate performance correlates with the relay amplification factor, the desired signals of users and the noise terms. Hence, we will investigate the deterministic results of all these terms as follows.

(a) Deterministic amplification factor:

$$\beta_{zf}=\sqrt{\frac{P_R}{\frac{P_U}{N}\rho\text{tr}\left(\bar{\mathbf{F}}_{zf}\mathbf{H}_{MAC}\mathbf{H}_{MAC}^H\bar{\mathbf{F}}_{zf}^H\right)+\rho\sigma_R^2\text{tr}\left(\bar{\mathbf{F}}_{zf}\bar{\mathbf{F}}_{zf}^H\right)+\sigma_{R,\,z}^2\text{tr}\left(\bar{\mathbf{F}}_{zf}\bar{\mathbf{F}}_{zf}^H\right)}}. \tag{10}$$

$$\beta_{zf}^2=\frac{P_RM^2}{\frac{P_U}{N}\rho M\underbrace{M\text{tr}\left(\bar{\mathbf{F}}_{zf}\mathbf{H}_{MAC}\mathbf{H}_{MAC}^H\bar{\mathbf{F}}_{zf}^H\right)}_{\Omega_{zf1}}+\left(\rho\sigma_R^2+\sigma_{R,\,z}^2\right)\underbrace{M^2\text{tr}\left(\bar{\mathbf{F}}_{zf}\bar{\mathbf{F}}_{zf}^H\right)}_{\Omega_{zf2}}} \tag{11}$$

By the definition of $\mathbf{F}_{zf}$, β_{zf}^2 can be rewritten as (11). Applying the trace property $\text{tr}(\mathbf{AB})=\text{tr}(\mathbf{BA})$ and (10), we can obtain

$$\begin{aligned}\Omega_{zf1}&=\text{tr}\left(M\mathbf{H}_{MAC}^H\bar{\mathbf{F}}_{zf}^H\bar{\mathbf{F}}_{zf}\mathbf{H}_{MAC}\right)\\&=\text{tr}\left(M\mathbf{T}^H\left(\mathbf{G}_{BC}\mathbf{G}_{BC}^H\right)^{-1}\mathbf{T}\right)\\&=\text{tr}\left(\mathbf{T}^H\left(\frac{\mathbf{G}_{BC}\mathbf{G}_{BC}^H}{M}\right)^{-1}\mathbf{T}\right).\end{aligned} \tag{12}$$

Future employing the definition of $\mathbf{G}_{BC}$, we achieve

$$\left(\frac{\mathbf{G}_{BC}\mathbf{G}_{BC}^H}{M}\right)^{-1}=\begin{pmatrix}\frac{\mathbf{G}_1\mathbf{G}_1^H}{M}&\frac{\mathbf{G}_1\mathbf{G}_2^H}{M}\\\frac{\mathbf{G}_2\mathbf{G}_1^H}{M}&\frac{\mathbf{G}_2\mathbf{G}_2^H}{M}\end{pmatrix}^{-1}. \tag{13}$$

With the law of large numbers [21], we get

$$\frac{\mathbf{G}_i\mathbf{G}_i^H}{M}\xrightarrow[M\to\infty]{a.s.}L_i\varphi_{ru_i}^2\mathbf{I}_N, \tag{14}$$

$$\frac{\mathbf{H}_i^H\mathbf{H}_i}{M}\xrightarrow[M\to\infty]{a.s.}L_i\varphi_{u_ir}^2\mathbf{I}_N, \tag{15}$$

where $\xrightarrow[M\to\infty]{a.s.}$ represents the convergence operation when M tends to infinity. Plugging (14) into (13), we achieve

$$\begin{aligned}\left(\frac{\mathbf{G}_{BC}\mathbf{G}_{BC}^H}{M}\right)^{-1}&\xrightarrow[M\to\infty]{a.s.}\begin{pmatrix}L_1\varphi_{ru_1}^2\mathbf{I}_N&\mathbf{0}_{N\times N}\\\mathbf{0}_{N\times N}&L_2\varphi_{ru_2}^2\mathbf{I}_N\end{pmatrix}^{-1}\\&=\begin{pmatrix}\left(L_1\varphi_{ru_1}^2\right)^{-1}\mathbf{I}_N&\mathbf{0}_{N\times N}\\\mathbf{0}_{N\times N}&\left(L_2\varphi_{ru_2}^2\right)^{-1}\mathbf{I}_N\end{pmatrix}.\end{aligned} \tag{16}$$

And, on the basis of (12) and (16), we obtain

$$\begin{aligned}&M\mathbf{H}_{MAC}^H\bar{\mathbf{F}}_{zf}^H\bar{\mathbf{F}}_{zf}\mathbf{H}_{MAC}\\&\xrightarrow[M\to\infty]{a.s.}\begin{pmatrix}\left(L_2\varphi_{ru_2}^2\right)^{-1}\mathbf{T}_2^H\mathbf{I}_N\mathbf{T}_2&\mathbf{0}_{N\times N}\\\mathbf{0}_{N\times N}&\left(L_1\varphi_{ru_1}^2\right)^{-1}\mathbf{T}_1^H\mathbf{I}_N\mathbf{T}_1\end{pmatrix}.\end{aligned} \tag{17}$$

Combining (17) and the trace property $\text{tr}(\mathbf{AB})=\text{tr}(\mathbf{BA})$, the deterministic result of Ω_{zf1} becomes (18) at the top of next page.

Substituting (8) into Ω_{zf2} further yields

$$\begin{aligned}\Omega_{zf2}&=M^2\text{tr}\left(\bar{\mathbf{F}}_{zf}^H\bar{\mathbf{F}}_{zf}\right)\\&=\text{tr}\left(\mathbf{T}^H\left(\frac{\mathbf{G}_{BC}\mathbf{G}_{BC}^H}{M}\right)^{-1}\mathbf{T}\left(\frac{\mathbf{H}_{MAC}^H\mathbf{H}_{MAC}}{M}\right)^{-1}\right).\end{aligned} \tag{19}$$

Based on (15), it is easy to obtain

$$\begin{aligned}\left(\frac{\mathbf{H}_{MAC}^H\mathbf{H}_{MAC}}{M}\right)^{-1}&=\begin{pmatrix}\frac{\mathbf{H}_1^H\mathbf{H}_1}{M}&\frac{\mathbf{H}_1^H\mathbf{H}_2}{M}\\\frac{\mathbf{H}_2^H\mathbf{H}_1}{M}&\frac{\mathbf{H}_2^H\mathbf{H}_2}{M}\end{pmatrix}^{-1}\\&\xrightarrow[M\to\infty]{a.s.}\begin{pmatrix}\left(L_1\varphi_{u_1r}^2\right)^{-1}\mathbf{I}_N&\mathbf{0}_{N\times N}\\\mathbf{0}_{N\times N}&\left(L_2\varphi_{u_2r}^2\right)^{-1}\mathbf{I}_N\end{pmatrix}.\end{aligned} \tag{20}$$

Substituting (16) and (20) back into (19), the deterministic result of Ω_{zf2} can be expressed as (21) at the top of next page.

Finally, using the results of (18) and (21), we achieve the deterministic amplification factor of ZFR/ZFT relay precoding as (22) at the tope of next page. It is noteworthy that $\widehat{\beta}_{zf}^2$ represents the deterministic state of β_{zf}^2 when M tends to infinity.

(b) Deterministic achievable sum-rate:

According to (6), we have

$$\mathbf{Q}_i=\beta_{zf}^2\left(\mathbf{G}_i\bar{\mathbf{F}}_{zf}\mathbf{H}_{\bar{i}}\right)\left(\mathbf{G}_i\bar{\mathbf{F}}_{zf}\mathbf{H}_{\bar{i}}\right)^H. \tag{23}$$

Through multiplying $\mathbf{G}_{BC}$ and $\mathbf{H}_{MAC}$ on the left and right sides of $\bar{\mathbf{F}}_{zf}$, respectively, we have

$$\mathbf{G}_{BC}\bar{\mathbf{F}}_{zf}\mathbf{H}_{MAC}=\begin{pmatrix}\mathbf{G}_1\bar{\mathbf{F}}_{zf}\mathbf{H}_1&\mathbf{G}_1\bar{\mathbf{F}}_{zf}\mathbf{H}_2\\\mathbf{G}_2\bar{\mathbf{F}}_{zf}\mathbf{H}_1&\mathbf{G}_2\bar{\mathbf{F}}_{zf}\mathbf{H}_2\end{pmatrix}. \tag{24}$$

Based on the definition of the ZFR/ZFT design, we achieve

$$\mathbf{G}_{BC}\bar{\mathbf{F}}_{zf}\mathbf{H}_{MAC}=\mathbf{T}=\begin{pmatrix}\mathbf{0}_{N\times N}&\mathbf{T}_1\\\mathbf{T}_2&\mathbf{0}_{N\times N}\end{pmatrix}. \tag{25}$$

With (24) and (25), we achieve $\mathbf{G}_i\mathbf{F}_{zf}\mathbf{H}_{\bar{i}}=\mathbf{T}_i$. The deterministic result of desired signal term is simplified as

$$\mathbf{Q}_i\xrightarrow[M\to\infty]{a.s.}\widehat{\beta}_{zf}^2\mathbf{T}_i\mathbf{T}_i^H. \tag{26}$$

From (6), the relay noise term can be written as

$$\mathbf{W}_i=\beta_{zf}^2\mathbf{G}_i\bar{\mathbf{F}}_{zf}\bar{\mathbf{F}}_{zf}^H\mathbf{G}_i^H. \tag{27}$$

The term $\bar{\mathbf{F}}_{zf}\bar{\mathbf{F}}_{zf}^H$ is multiplied by $\mathbf{G}_{BC}$ and $\mathbf{G}_{BC}^H$ at the left and right hand sides, respectively. Then, we obtain

$$\begin{aligned}\mathbf{G}_{BC}\bar{\mathbf{F}}_{zf}\bar{\mathbf{F}}_{zf}^H\mathbf{G}_{BC}^H&=\mathbf{T}\left(\mathbf{H}_{MAC}^H\mathbf{H}_{MAC}\right)^{-1}\mathbf{T}^H\\&=\frac{1}{M}\mathbf{T}\left(\frac{\mathbf{H}_{MAC}^H\mathbf{H}_{MAC}}{M}\right)^{-1}\mathbf{T}^H.\end{aligned} \tag{28}$$

Substituting (20) into (28), we have the deterministic result of $\mathbf{G}_{BC}\bar{\mathbf{F}}_{zf}\bar{\mathbf{F}}_{zf}^H\mathbf{G}_{BC}^H$ as

$$\begin{aligned}&\mathbf{G}_{BC}\bar{\mathbf{F}}_{zf}\bar{\mathbf{F}}_{zf}^H\mathbf{G}_{BC}^H\\&\xrightarrow[M\to\infty]{a.s.}\frac{1}{M}\begin{pmatrix}\mathbf{T}_1\left(L_2\varphi_{u_2r}^2\right)^{-1}\mathbf{I}_N\mathbf{T}_1^H&\mathbf{0}_{N\times N}\\\mathbf{0}_{N\times N}&\mathbf{T}_2\left(L_1\varphi_{u_1r}^2\right)^{-1}\mathbf{I}_N\mathbf{T}_2^H\end{pmatrix}.\end{aligned} \tag{29}$$

$$\Omega_{zf1} = \mathrm{tr}\left(M\mathbf{H}_{MAC}^H\bar{\mathbf{F}}_R^H\bar{\mathbf{F}}_R\mathbf{H}_{MAC}\right) \xrightarrow[M\to\infty]{a.s.} \left(L_2\varphi_{ru_2}^2\right)^{-1}\mathrm{tr}\left(\mathbf{T}_2^H\mathbf{I}_N\mathbf{T}_2\right) + \left(L_1\varphi_{ru_1}^2\right)^{-1}\mathrm{tr}\left(\mathbf{T}_1^H\mathbf{I}_N\mathbf{T}_1\right)$$
$$= \frac{N}{L_2\varphi_{ru_2}^2} + \frac{N}{L_1\varphi_{ru_1}^2} = \frac{N\left(L_1\varphi_{ru_1}^2 + L_2\varphi_{ru_2}^2\right)}{L_1L_2\varphi_{ru_1}^2\varphi_{ru_2}^2} \tag{18}$$

$$\Omega_{zf2} \xrightarrow[M\to\infty]{a.s.} \mathrm{tr}\left(\mathbf{T}^H\begin{pmatrix}\left(L_1\varphi_{ru_1}^2\right)^{-1}\mathbf{I}_N & \mathbf{0}_{N\times N}\\ \mathbf{0}_{N\times N} & \left(L_2\varphi_{ru_2}^2\right)^{-1}\mathbf{I}_N\end{pmatrix}\mathbf{T}\begin{pmatrix}\left(L_1\varphi_{u_1r}^2\right)^{-1}\mathbf{I}_N & \mathbf{0}_{N\times N}\\ \mathbf{0}_{N\times N} & \left(L_2\varphi_{u_2r}^2\right)^{-1}\mathbf{I}_N\end{pmatrix}\right)$$
$$= \mathrm{tr}\begin{pmatrix}\left(L_1L_2\varphi_{u_1r}^2\varphi_{ru_2}^2\right)^{-1}\mathbf{T}_2^H\mathbf{I}_N\mathbf{T}_2\mathbf{I}_N & \mathbf{0}_{N\times N}\\ \mathbf{0}_{N\times N} & \left(L_1L_2\varphi_{u_2r}^2\varphi_{ru_1}^2\right)^{-1}\mathbf{T}_1^H\mathbf{I}_N\mathbf{T}_1\mathbf{I}_N\end{pmatrix} = \sum_{i=1}^{2}\frac{N}{L_iL_{\bar{i}}\varphi_{u_ir}^2\varphi_{ru_{\bar{i}}}^2} \tag{21}$$

$$\beta_{zf}^2 \xrightarrow[M\to\infty]{a.s.} \widehat{\beta}_{zf}^2 = \frac{P_RM^2}{\frac{P_U\rho M\left(L_1\varphi_{ru_1}^2+L_2\varphi_{ru_2}^2\right)}{L_1L_2\varphi_{ru_1}^2\varphi_{ru_2}^2} + \left(\rho\sigma_R^2+\sigma_{R,\,z}^2\right)\left(\sum_{i=1}^{2}\frac{N}{L_iL_{\bar{i}}\varphi_{u_ir}^2\varphi_{ru_{\bar{i}}}^2}\right)}. \tag{22}$$

$$\widehat{R}_{sum,zf} = \sum\nolimits_{i=1}^{2}\frac{1}{2}\log_2\det\left\{\mathbf{I}_N + \left[\frac{P_U}{N}\rho\widehat{\beta}_{zf}^2\mathbf{T}_i\mathbf{T}_i^H\right]\left[\left(\rho\sigma_R^2+\sigma_{R,\,z}^2\right)\frac{\widehat{\beta}_{zf}^2}{ML_{\bar{i}}\varphi_{u_{\bar{i}}r}^2}\mathbf{T}_i\mathbf{I}_N\mathbf{T}_i^H + \sigma_i^2\mathbf{I}_N\right]^{-1}\right\}. \tag{33}$$

Meanwhile, due to the definition of $\mathbf{G}_{BC}$, (28) can be rewritten as

$$\mathbf{G}_{BC}\bar{\mathbf{F}}_{zf}\bar{\mathbf{F}}_{zf}^H\mathbf{G}_{BC}^H = \begin{pmatrix}\mathbf{G}_1\\ \mathbf{G}_2\end{pmatrix}\bar{\mathbf{F}}_{zf}\bar{\mathbf{F}}_{zf}^H\begin{pmatrix}\mathbf{G}_1^H & \mathbf{G}_2^H\end{pmatrix}$$
$$= \begin{pmatrix}\mathbf{G}_1\bar{\mathbf{F}}_{zf}\bar{\mathbf{F}}_{zf}^H\mathbf{G}_1^H & \mathbf{G}_1\bar{\mathbf{F}}_{zf}\bar{\mathbf{F}}_{zf}^H\mathbf{G}_2^H\\ \mathbf{G}_2\bar{\mathbf{F}}_{zf}\bar{\mathbf{F}}_{zf}^H\mathbf{G}_1^H & \mathbf{G}_2\bar{\mathbf{F}}_{zf}\bar{\mathbf{F}}_{zf}^H\mathbf{G}_2^H\end{pmatrix}. \tag{30}$$

From (29) and (30), it reveals obviously that

$$\mathbf{G}_i\bar{\mathbf{F}}_{zf}\bar{\mathbf{F}}_{zf}^H\mathbf{G}_i^H \xrightarrow[M\to\infty]{a.s.} \frac{1}{M}\mathbf{T}_i\left(L_{\bar{i}}\varphi_{u_{\bar{i}}r}^2\right)^{-1}\mathbf{I}_N\mathbf{T}_i^H. \tag{31}$$

Thus, the deterministic result of relay noise term becomes

$$\mathbf{W}_i \xrightarrow[M\to\infty]{a.s.} \frac{\widehat{\beta}_{zf}^2}{M}\mathbf{T}_i\left(L_{\bar{i}}\varphi_{u_{\bar{i}}r}^2\right)^{-1}\mathbf{I}_N\mathbf{T}_i^H. \tag{32}$$

Putting (26) and (32) into (7), the deterministic achievable sum-rate with ZFR/ZFT relay precoding is derived as (33) at the top of this page.

Following the similar way, the deterministic result of the term E_R is approximated as

$$E_R \xrightarrow[M\to\infty]{a.s.} \widehat{E}_R = \eta\left(1-\rho\right)MP_U\left(\sum_{i=1}^{2}L_i\varphi_{u_1r}^2\right). \tag{34}$$

It is noteworthy that $\widehat{E}_R$ is not relevant to the relay precoding design.

B. Deterministic sum-rate with MRC/MRT relay precoding

1) MRC/MRT processing at the relay: The low-complexity MRC/MRT processing is adopted at the relay node and the precoding matrix is given by $\mathbf{F}_{mr} = \beta_{mr}\bar{\mathbf{F}}_{mr}$, where β_{mr} is the amplification factor with MRC/MRT relay precoding. Based on [20], [22], $\bar{\mathbf{F}}_{mr}$ is formulated as

$$\bar{\mathbf{F}}_{mr} = \mathbf{G}_{BC}^H\mathbf{T}\mathbf{H}_{MAC}^H = \sum_{j=1}^{2}\mathbf{G}_{\bar{j}}^H\mathbf{T}_{\bar{j}}\mathbf{H}_j^H. \tag{35}$$

2) Deterministic sum-rate with MRC/MRT relay precoding: (a) Deterministic amplification factor:

Similar to the ZFR/ZFT precoding scheme, the relay amplification factor with MRC/MRT precoding can be written as (36) at the top of next page.

Before deriving the deterministic result of relay amplification factor with MRC/MRT processing, one vital proposition is provided as follows.

Proposition 1. *For two independent and identically matrices* $\mathbf{X} \sim \mathbb{CN}_{N,M}\left(0, \tau^2\mathbf{I}_N \otimes \mathbf{I}_M\right)$, $\mathbf{Y} \sim \mathbb{CN}_{N,M}\left(0, \tau^2\mathbf{I}_N \otimes \mathbf{I}_M\right)$, *we have*

$$\frac{1}{M}\mathbf{X}\mathbf{X}^H \xrightarrow[M\to\infty]{a.s.} \tau^2\mathbf{I}_N,\ \frac{1}{M}\mathbf{X}\mathbf{Y}^H \xrightarrow[M\to\infty]{a.s.} \mathbf{0}_N. \tag{37}$$

Proof. The result of Proposition 1 can be obtained by the extension of Lemma 1 in [22]. ■

According to (35) and $\mathrm{tr}\left(\mathbf{AB}\right) = \mathrm{tr}\left(\mathbf{BA}\right)$, we achieve

$$\frac{1}{M^3}\Omega_{mr1} = \sum_{i=1}^{2}\sum_{j=1}^{2}\sum_{k=1}^{2}\mathrm{tr}\left(\frac{\mathbf{G}_{\bar{k}}\mathbf{G}_{\bar{j}}^H}{M}\mathbf{T}_{\bar{j}}\frac{\mathbf{H}_j^H\mathbf{H}_i}{M}\frac{\mathbf{H}_i^H\mathbf{H}_k}{M}\mathbf{T}_{\bar{k}}^H\right). \tag{38}$$

With (14), (15) and Proposition 1, the following result can be obtained

$$\frac{1}{M^3}\Omega_{mr1} \xrightarrow[M\to\infty]{a.s.} \sum_{i=1}^{2}L_{\bar{i}}L_i^2\varphi_{ru_{\bar{i}}}^2\varphi_{u_ir}^4\mathrm{tr}\left(\mathbf{T}_{\bar{i}}\mathbf{T}_{\bar{i}}^H\right). \tag{39}$$

Applying the same approach, we have

$$\frac{1}{M^2}\Omega_{mr2} = \sum_{i=1}^{2}\sum_{j=1}^{2}\mathrm{tr}\left(\frac{\mathbf{G}_{\bar{j}}\mathbf{G}_{\bar{i}}^H}{M}\mathbf{T}_{\bar{j}}\frac{\mathbf{H}_i^H\mathbf{H}_j}{M}\mathbf{T}_{\bar{k}}^H\right)$$
$$\xrightarrow[M\to\infty]{a.s.} \sum_{i=1}^{2}L_{\bar{i}}L_i\varphi_{ru_{\bar{i}}}^2\varphi_{u_ir}^2\mathrm{tr}\left(\mathbf{T}_{\bar{i}}\mathbf{T}_{\bar{i}}^H\right). \tag{40}$$

$$\beta_{mr}^2 = \frac{P_R}{\frac{P_U}{N}\rho\sum_{i=1}^{2}\underbrace{\mathrm{tr}\left(\bar{\mathbf{F}}_{mr}\mathbf{H}_i\mathbf{H}_i^H\bar{\mathbf{F}}_{mr}^H\right)}_{\Omega_{mr1}} + \left(\rho\sigma_R^2+\sigma_{R,\,z}^2\right)\underbrace{\mathrm{tr}\left(\bar{\mathbf{F}}_{mr}\bar{\mathbf{F}}_{mr}^H\right)}_{\Omega_{mr2}}}. \tag{36}$$

$$\beta_{mr}^2 \xrightarrow[M\to\infty]{a.s.} \widehat{\beta}_{mr}^2 = \frac{P_R}{P_U\rho M^3\left(\sum\limits_{i=1}^{2}L_{\bar{i}}L_i^2\varphi_{ru_{\bar{i}}}^2\varphi_{u_ir}^4\right) + \left(\rho\sigma_R^2+\sigma_{R,\,z}^2\right)M^2N\left(\sum\limits_{i=1}^{2}L_{\bar{i}}L_i\varphi_{ru_{\bar{i}}}^2\varphi_{u_ir}^2\right)}. \tag{41}$$

$$\widehat{R}_{sum,mr} = \sum\nolimits_{i=1}^{2}\frac{1}{2}\log_2\det\left\{\mathbf{I}_N + \left[\frac{P_U}{N}\rho M^4\widehat{\beta}_{mr}^2L_i^2L_{\bar{i}}^2\varphi_{ru_i}^4\varphi_{u_{\bar{i}}r}^4\mathbf{T}_i\mathbf{T}_i^H\right] \times\left[\left(\rho\sigma_R^2+\sigma_{R,\,z}^2\right)M^3\widehat{\beta}_{mr}^2L_i^2L_{\bar{i}}\varphi_{ru_i}^4\varphi_{u_{\bar{i}}r}^2\mathbf{T}_i\mathbf{T}_i^H+\sigma_i^2\mathbf{I}_N\right]^{-1}\right\}. \tag{45}$$

Substituting (39) and (40) back into (36), we achieve the deterministic amplification factor of MRC/MRT relay precoding as (41) at the top of this page.

(b) Deterministic achievable sum-rate:

According to the precoding matrix $\mathbf{F}_{mr}$, we can transform the desired signal term into

$$\frac{1}{M^4}\mathbf{Q}_i = \beta_{mr}^2\sum_{j=1}^{2}\sum_{k=1}^{2}\frac{\mathbf{G}_i\mathbf{G}_{\bar{j}}^H}{M}\mathbf{T}_{\bar{j}}\frac{\mathbf{H}_{\bar{j}}^H\mathbf{H}_{\bar{i}}}{M}\frac{\mathbf{H}_{\bar{i}}^H\mathbf{H}_k}{M}\mathbf{T}_{\bar{k}}^H\frac{\mathbf{G}_{\bar{k}}\mathbf{G}_i^H}{M}. \tag{42}$$

Based on (14), (15) and Proposition 1, the deterministic result of (42) can be expressed as

$$\frac{1}{M^4}\mathbf{Q}_i \xrightarrow[M\to\infty]{a.s.} \widehat{\beta}_{mr}^2L_i^2L_{\bar{i}}^2\varphi_{ru_i}^4\varphi_{u_{\bar{i}}r}^4\mathbf{T}_i\mathbf{T}_i^H. \tag{43}$$

By further deriving the deterministic result of noise term with the similar way, we achieve

$$\frac{1}{M^3}\mathbf{W}_i = \beta_{mr}^2\sum_{j=1}^{2}\sum_{k=1}^{2}\frac{\mathbf{G}_i\mathbf{G}_{\bar{j}}^H}{M}\mathbf{T}_{\bar{j}}\frac{\mathbf{H}_{\bar{j}}^H\mathbf{H}_k}{M}\mathbf{T}_{\bar{k}}^H\frac{\mathbf{G}_{\bar{k}}\mathbf{G}_i^H}{M} \xrightarrow[M\to\infty]{a.s.} \widehat{\beta}_{mr}^2L_i^2L_{\bar{i}}\varphi_{ru_{\bar{i}}}^4\varphi_{u_{\bar{i}}r}^2\mathbf{T}_i\mathbf{T}_i^H. \tag{44}$$

Plugging (43)and (44) into (7), the deterministic achievable sum-rate with MRC/MRT relay precoding becomes (45) at the top of this page.

IV. Transmission power scaling with ZFR/ZFT relay precoding

In this section, the deterministic sum-rate is future investigated under different power scaling laws. Under some power scaling cases, the deterministic sum-rate approaches a ceiling when the number of relay antennas grows to infinity [22]. This ceiling is defined as the asymptotic rate in this paper. Similar to [20], the achievable sum-rates of four prevalent power scaling cases with ZFR/ZFT relay precoding are investigated, as shown in Table I. It is noteworthy that the power factor of user $\widehat{E}_U$ is fixed and unrelated with M and $\widehat{E}_R$ has been stated in (34). When $M\to\infty$, we have the following details of the asymptotic rate analysis.

A. Case 1: $P_U = \widehat{E}_U$, $P_R = \widehat{E}_R$

Proposition 2. *In this case, the received signal at U_i satisfies*

$$\frac{\mathbf{y}_i}{M} \xrightarrow[M\to\infty]{a.s.} \sqrt{\frac{\widehat{E}_{RC}L_1L_2\varphi_{ru_1}^2\varphi_{ru_2}^2}{N\left(L_1\varphi_{ru_1}^2+L_2\varphi_{ru_2}^2\right)}}\mathbf{T}_i\mathbf{x}_{\bar{i}}, \tag{46}$$

where $\widehat{E}_{RC} = \eta\left(1-\rho\right)E_U\left(\sum\limits_{i=1}^{2}L_i\varphi_{u_1r}^2\right)$ is one constant which is irrelevant to M.

Proof. Refer to Appendix A. ■

From (46), we can conclude that the asymptotic sum-rate of Case 1 tends to infinity. Obviously, when M goes to infinity, the power splitting and common noise at the relay, the noise and self-interference at two users all disappear. The reason

TABLE I: The asymptotic sum-rates of four power scaling cases with ZFR/ZFT relay precoding

Case	Power of each user	Power of relay	Asymptotic sum-rate: ZFR/ZFT($M\to\infty$)
1	$P_U = \widehat{E}_U$	$P_R = \widehat{E}_R$	∞
2	$P_U = \widehat{E}_U$	$P_R = \widehat{E}_R\Big/M$	∞
3	$P_U = \widehat{E}_U\Big/M$	$P_R = \widehat{E}_R$	$\frac{N}{2}\sum\limits_{i=1}^{2}\log_2\left(1+\frac{\widehat{E}_U\rho L_{\bar{i}}\varphi_{u_{\bar{i}}r}^2}{\left(\rho\sigma_R^2+\sigma_{R,\,z}^2\right)N}\right)$
4	$P_U = \widehat{E}_U\Big/M$	$P_R = \widehat{E}_R\Big/M$	$\frac{N}{2}\sum\limits_{i=1}^{2}\log_2\left(1+\frac{\widehat{E}_U\rho\widehat{E}_{RC}L_{\bar{i}}\varphi_{u_{\bar{i}}r}^2}{N\left[\left(\rho\sigma_R^2+\sigma_{R,\,z}^2\right)\widehat{E}_{RC}+L_{\bar{i}}\varphi_{u_{\bar{i}}r}^2\omega_{zf}\sigma_{\bar{i}}^2\right]}\right)$

$$\widehat{R}_{sum,zf} = \frac{1}{2}\sum\nolimits_{i=1}^{2} \log_2 \det \left\{ \mathbf{I}_N + \left[\frac{\widehat{E}_U}{NM} \rho \widehat{\beta}_{zf}^{\,2} \mathbf{T}_i \mathbf{T}_i^H \right] \left[\frac{\left(\rho\sigma_R^2 + \sigma_{R,\,z}^2\right) \widehat{\beta}_{zf}^{\,2}}{M L_{\bar{i}} \varphi_{u_{\bar{i}}r}^2} \mathbf{T}_i \mathbf{I}_N \mathbf{T}_i^H + \sigma_i^2 \mathbf{I}_N \right]^{-1} \right\}, \tag{48}$$

$$\widehat{\beta}_{zf} = \sqrt{\frac{\widehat{E}_{RC} M^2}{\frac{\widehat{E}_{RC}\rho\left(L_1\varphi_{ru_1}^2 + L_2\varphi_{ru_2}^2\right)}{L_1 L_2 \varphi_{ru_1}^2 \varphi_{ru_2}^2} + \left(\rho\sigma_R^2 + \sigma_{R,\,z}^2\right)\left(\sum\limits_{i=1}^{2} \frac{N}{L_i L_{\bar{i}} \varphi_{u_i r}^2 \varphi_{ru_{\bar{i}}}^2}\right)}}. \tag{49}$$

$$\widehat{R}_{sum,zf}^{\infty} = \lim_{M\to\infty} \widehat{R}_{sum,zf} = \frac{N}{2}\sum_{i=1}^{2} \log_2 \left(1 + \frac{\widehat{E}_U \rho \widehat{E}_{RC} L_{\bar{i}} \varphi_{u_{\bar{i}}r}^2}{N\left[\left(\rho\sigma_R^2 + \sigma_{R,\,z}^2\right)\widehat{E}_{RC} + L_{\bar{i}}\varphi_{u_{\bar{i}}r}^2 \omega_{zf}\sigma_i^2\right]} \right). \tag{52}$$

$$\begin{aligned} \widehat{R}_{sum,mr} =& \frac{1}{2}\sum\nolimits_{i=1}^{2} \log_2 \det \left\{ \mathbf{I}_N + \left[\frac{\widehat{E}_U}{N} \rho M^3 \widehat{\beta}_{mr}^{\,2} L_i^2 L_{\bar{i}}^2 \varphi_{ru_i}^4 \varphi_{u_{\bar{i}}r}^4 \mathbf{T}_i \mathbf{T}_i^H \right] \right. \\ & \left. \times \left[\left(\rho\sigma_R^2 + \sigma_{R,\,z}^2\right) M^3 \widehat{\beta}_{mr}^{\,2} L_i^2 L_{\bar{i}} \varphi_{ru_i}^4 \varphi_{u_{\bar{i}}r}^2 \mathbf{T}_i \mathbf{T}_i^H + \sigma_i^2 \mathbf{I}_N \right]^{-1} \right\}. \end{aligned} \tag{55}$$

$$\widehat{\beta}_{mr} = \sqrt{\frac{\widehat{E}_{RC}}{\widehat{E}_U \rho M^2 \left(\sum\limits_{i=1}^{2} L_{\bar{i}} L_i^2 \varphi_{ru_{\bar{i}}}^2 \varphi_{u_i r}^4\right) + \left(\rho\sigma_R^2 + \sigma_{R,\,z}^2\right) M^2 N \left(\sum\limits_{i=1}^{2} L_{\bar{i}} L_i \varphi_{ru_{\bar{i}}}^2 \varphi_{u_i r}^2\right)}}. \tag{56}$$

$$\widehat{R}_{sum,mr}^{\infty} = \lim_{M\to\infty} \widehat{R}_{sum,mr} = \frac{N}{2}\sum_{i=1}^{2} \log_2 \left(1 + \frac{\widehat{E}_U \rho \widehat{E}_{RC} L_i^2 L_{\bar{i}}^2 \varphi_{ru_i}^4 \varphi_{u_{\bar{i}}r}^4}{N\left[\left(\rho\sigma_R^2 + \sigma_{R,\,z}^2\right)\widehat{E}_{RC} L_i^2 L_{\bar{i}} \varphi_{ru_i}^4 \varphi_{u_{\bar{i}}r}^2 + \omega_{mr}\sigma_i^2\right]} \right). \tag{59}$$

for this is that the MIMO channels of both sides of relay change more orthogonal as M increases. Moreover, due to the unlimited increase of harvested energy, the transmission power of relay goes to infinity when $M \to \infty$.

B. Case 2: $P_U = \widehat{E}_U$, $P_R = \widehat{E}_R \Big/ M$

Proposition 3. *In Case 2, the received signal term at U_i when $M \to \infty$, is given by*

$$\frac{\mathbf{y}_i}{\sqrt{M}} \xrightarrow[M\to\infty]{a.s.} \sqrt{\frac{\widehat{E}_{RC} L_1 L_2 \varphi_{ru_1}^2 \varphi_{ru_2}^2}{N\left(L_1\varphi_{ru_1}^2 + L_2\varphi_{ru_2}^2\right)}} \mathbf{T}_i \mathbf{x}_{\bar{i}}. \tag{47}$$

Proof. Refer to Appendix B. ∎

Similar to Case 1, the asymptotic rate of Case 2 tends to infinity as M increases. However, the transmission power of relay that is supplied by the harvested energy approaches to $\widehat{E}_{RC}$, when $M \to \infty$. From (47), we also discover that all the interference and noise are diluted to zero when M is large enough.

C. Case 3: $P_U = \widehat{E}_U \Big/ M$, $P_R = \widehat{E}_R$

Substituting the transmission power scaling of Case 3 into (33), the deterministic achievable sum-rate is re-expressed as (48) with $\widehat{\beta}_{zf}$ being (49) at the top of this page.

The asymptotic result of the deterministic sum-rate when $M \to \infty$ is represented as

$$\begin{aligned} \widehat{R}_{sum,zf}^{\infty} &= \lim_{M\to\infty} \widehat{R}_{sum,zf} \\ &= \frac{N}{2}\sum_{i=1}^{2} \log_2 \left(1 + \frac{\widehat{E}_U \rho L_{\bar{i}} \varphi_{u_{\bar{i}}r}^2}{\left(\rho\sigma_R^2 + \sigma_{R,\,z}^2\right) N} \right). \end{aligned} \tag{50}$$

From (50), it is noted that the asymptotic rate of Case 3 approaches to a ceiling rather than reduces to zero when the transmission power of users are scaled down to $1/M$. The main reason for this is that the relay system can obtain diversity gain from the massive antennas. Likewise, the PS factor has a great effect on the asymptotic sum-rate. Besides, the transmission power of relay tends to $\widehat{E}_{RC}$ when $M \to \infty$. We also observe that the noise term at users can be diluted to zero when M approaches to infinity, whereas the noise from relay still exists. Likewise, the asymptotic sum-rate of Case 3 increases as N grows in non-linear model.

D. Case 4: $P_U = \widehat{E}_U \Big/ M$, $P_R = \widehat{E}_R \Big/ M$

Plugging the transmission power scaling of Case 4 into (33), the deterministic achievable sum-rate is also represented by

(48), with $\widehat{\beta}_{zf}$ as

$$\widehat{\beta}_{zf} = \sqrt{\frac{\widehat{E}_{RC} M}{\widehat{E}_U \rho a_{zf} + \left(\rho \sigma_R^2 + \sigma_{R,\,z}^2\right) N b_{zf}}}, \tag{51}$$

where $a_{zf} = \frac{\left(L_1 \varphi_{ru_1}^2 + L_2 \varphi_{ru_2}^2\right)}{L_1 L_2 \varphi_{ru_1}^2 \varphi_{ru_2}^2}$ and $b_{zf} = \sum_{i=1}^{2} \frac{1}{L_i L_{\bar{i}} \varphi_{u_i r}^2 \varphi_{ru_{\bar{i}}}^2}$. Meanwhile, future defining $\omega_{zf} \triangleq \widehat{E}_U \rho a_{zf} + \left(\rho \sigma_R^2 + \sigma_{R,\,z}^2\right) N b_{zf}$. With (48) and (51), the asymptotic result of deterministic achievable sum-rate when M tends to infinity is given by (52) at the top of last page.

Equation (52) depicts that the asymptotic rate of Case 4 goes to a constant value when the number of relay antennas goes to infinite. Distinguishing from Case 3, the transmission power is equivalent to $\widehat{E}_{RC} \Big/ M$. Moreover, the noise at two users and the relay node cannot be eliminated as M increases to infinity. According to (52), the tendency of the asymptotic result in Case 4 is dubious as N grows.

V. Transmission power scaling with MRC/MRT relay precoding

In this section, the achievable sum-rates of four main power scaling cases with MRC/MRT relay precoding are investigated when the number of relay antennas goes to infinity, as shown in Table II.

A. Case 1: $P_U = \widehat{E}_U$, $P_R = \widehat{E}_R$

Proposition 4. *In this case, with MRC/MRT relay precoding, the received signal at U_i satisfies*

$$\frac{\mathbf{y}_i}{M} \xrightarrow[M\to\infty]{a.s.} \sqrt{\frac{\widehat{E}_{RC} L_i^2 L_{\bar{i}}^2 \varphi_{ru_i}^4 \varphi_{u_{\bar{i}} r}^4}{N\left(\sum_{i=1}^{2} L_{\bar{i}} L_i^2 \varphi_{ru_{\bar{i}}}^2 \varphi_{u_i r}^4\right)}} \mathbf{T}_i \mathbf{x}_{\bar{i}}. \tag{53}$$

Proof. Refer to Appendix C. ∎

Similar to ZFR/ZFT precoding, the asymptotic rate approaches to infinity with the growth of M. We also find that all interference and noise are eliminated. Besides, the transmission power at the relay tends to infinity as $M \to \infty$.

B. Case 2: $P_U = \widehat{E}_U$, $P_R = \widehat{E}_R \Big/ M$

Proposition 5. *In this case, with MRC/MRT relay precoding, the received signal at U_i satisfies*

$$\frac{\mathbf{y}_i}{\sqrt{M}} \xrightarrow[M\to\infty]{a.s.} \sqrt{\frac{\widehat{E}_{RC} L_i^2 L_{\bar{i}}^2 \varphi_{ru_i}^4 \varphi_{u_{\bar{i}} r}^4}{N\left(\sum_{i=1}^{2} L_{\bar{i}} L_i^2 \varphi_{ru_{\bar{i}}}^2 \varphi_{u_i r}^4\right)}} \mathbf{T}_i \mathbf{x}_{\bar{i}}. \tag{54}$$

Proof. Refer to Appendix D. ∎

Similar asymptotic performance can be obtained from Proposition 5. The asymptotic rate of Case 2 with MRC/MRT precoding also approaches to infinity as $M \to \infty$. Moreover, the useless influence of all the interference and noise is averaged to zero when M goes to infinity, whereas the transmission of relay approaches to a fixed value $\widehat{E}_{RC}$.

C. Case 3: $P_U = \widehat{E}_U \Big/ M$, $P_R = \widehat{E}_R$

Substituting the transmission power scaling of Case 3 into (45), the deterministic achievable sum-rate is re-expressed as (55) with $\widehat{\beta}_{mr}$ being (56) at the top of last page.

The asymptotic result of deterministic sum-rate when $M \to \infty$ is represented as

$$\begin{aligned} \widehat{R}_{sum,mr}^{\infty} &= \lim_{M\to\infty} \widehat{R}_{sum,mr} \\ &= \frac{N}{2} \sum_{i=1}^{2} \log_2 \left(1 + \frac{\widehat{E}_U \rho L_{\bar{i}} \varphi_{u_{\bar{i}} r}^2}{\left(\rho \sigma_R^2 + \sigma_{R,\,z}^2\right) N}\right). \end{aligned} \tag{57}$$

Obviously, the relay system with MRC/MRT precoding has the same asymptotic sum-rate as that with ZFR/ZFT precoding in Case 3. Equation (57) also indicates that PS factor has huge influence upon the asymptotic sum-rate. Moreover, we can observe that the asymptotic sum-rate increases with the growth of N, whereas it is not with linear model.

D. Case 4: $P_U = \widehat{E}_U \Big/ M$, $P_R = \widehat{E}_R \Big/ M$

Plugging the transmission power scaling of Case 4 into (45), the deterministic achievable sum-rate is also represented by (55), with $\widehat{\beta}_{mr}$ as

$$\widehat{\beta}_{mr} = \sqrt{\frac{\widehat{E}_{RC}}{\widehat{E}_U \rho a_{mr} M^3 + \left(\rho \sigma_R^2 + \sigma_{R,\,z}^2\right) b_{mr} N M^3}}, \tag{58}$$

TABLE II: The asymptotic sum-rates of four power scaling cases with MRC/MRT relay precoding

Case	Power of each user	Power of relay	Asymptotic sum-rate: MRC/MRT ($M \to \infty$)
1	$P_U = \widehat{E}_U$	$P_R = \widehat{E}_R$	∞
2	$P_U = \widehat{E}_U$	$P_R = \widehat{E}_R \Big/ M$	∞
3	$P_U = \widehat{E}_U \Big/ M$	$P_R = \widehat{E}_R$	$\frac{N}{2} \sum_{i=1}^{2} \log_2 \left(1 + \frac{\widehat{E}_U \rho L_{\bar{i}} \varphi_{u_{\bar{i}} r}^2}{\left(\rho \sigma_R^2 + \sigma_{R,\,z}^2\right) N}\right)$
4	$P_U = \widehat{E}_U \Big/ M$	$P_R = \widehat{E}_R \Big/ M$	$\frac{N}{2} \sum_{i=1}^{2} \log_2 \left(1 + \frac{\widehat{E}_U \rho \widehat{E}_{RC} L_i^2 L_{\bar{i}}^2 \varphi_{ru_i}^4 \varphi_{u_{\bar{i}} r}^4}{N\left[\left(\rho \sigma_R^2 + \sigma_{R,\,z}^2\right) \widehat{E}_{RC} L_i^2 L_{\bar{i}} \varphi_{ru_i}^4 \varphi_{u_{\bar{i}} r}^2 + \omega_{mr} \sigma_{\bar{i}}^2\right]}\right)$

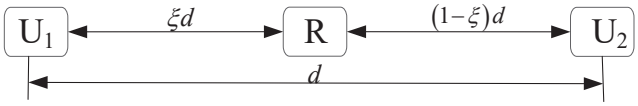

Fig. 2: The placement of massive MIMO two-way relay system.

where $a_{mr} = \sum_{i=1}^{2} L_{\bar{i}} L_i^2 \varphi_{ru_{\bar{i}}}^2 \varphi_{u_i r}^4$ and $b_{mr} = \sum_{i=1}^{2} L_{\bar{i}} L_i \varphi_{ru_{\bar{i}}}^2 \varphi_{u_i r}^2$. And, future defining $\omega_{mr} = \widehat{E}_U \rho a_{mr} + \left(\rho \sigma_R^2 + \sigma_{R,z}^2\right) N b_{mr}$. With (55) and (58), the asymptotic result of deterministic achievable sum-rate when M tends to infinity is given by (59) at the top of last page.

As shown in (59), the asymptotic rate of Case 4 with MRC/MRT precoding is similar to that of Case 4 with ZFR/ZFT. Both of them approaches to a constant value when $M \to \infty$. Besides, the asymptotic performance is also uncertain with the growth of N.

VI. Simulation and Numerical Results

In this section, extensive simulation results are provided to discuss the rate performance of massive MIMO two-way relaying system with SWIPT. As is well illustrated in Fig. 2, three transceivers in the two-way relay system are arranged in one line. We set the distance from U_1 to U_2, i.e., $d = 40$ meters, and denote $U_1 - R$ and $R - U_2$ distances as $d_1 = \xi d$ meters and $d_2 = (1-\xi)\, d$ meters, respectively. $\xi \in (0,\ 1)$ is the placement ratio of R in the relay system. Following [26], [29], [31], we model the large-scale fading as $L_i = \vartheta d_i^{-2}$, where 2 strands for the path loss exponent and ϑ is the condition parameter. Besides, all variances of the small-scale fading are set as $\varphi_{u_i r}^2 = \varphi_{r u_i}^2 = 1,\ i = 1, 2$. Unless otherwise explained, the noise variances at all transceivers are same as $\sigma_R^2 = \sigma_{R,z}^2 = \sigma_i^2 = \sigma^2 = -50$ dBm. We also specify $\eta = 0.8$, $\xi = 0.5$, $N = 2$, $T = 1$, $\vartheta = 1$, and $\widehat{E}_U = 10$ dBm.

In Fig. 3, the achievable sum-rate of the relay system versus the number of relay antennas M is provided for different power scaling cases. As expected, the theoretical analysis of sum-rates matches well with the real instantaneous sum-rates in various cases. It is intuitive that the sum-rates of four power scaling cases increase as M goes to infinity, the sum-rates of Case 1 and 2 grow unboundedly, whereas the sum-rates of Case 3 and 4 converge the corresponding asymptotic sum-rates. As can be observed in Fig. 3 (a), the covergence speed is $\mathcal{O}\left(\frac{1}{\sqrt{M}}\right)$ for Case 3 but $\mathcal{O}\left(\frac{1}{M}\right)$ for Case 4. Furthermore, if M is small, e.g., $M = 5$, the sum-rates of all four cases with MRC/MRT relay precoding are better than those with ZFR/ZFT relay precoding. This happens because for ZFR/ZFT relay precoding, forcing the MIMO channel to be orthogonal leads to the noise enhancement effect on the relay system when M is small. As mentioned above, these are consistent with the simulation results in [20], [22]. Besides, when M is large enough such as $M = 200$, two precodings have

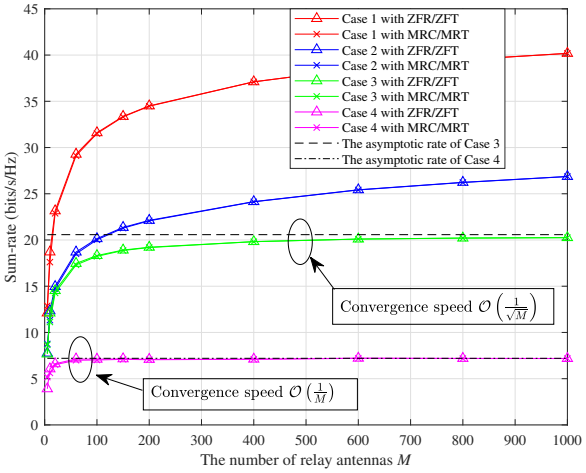

(a) $\vartheta = 3$.

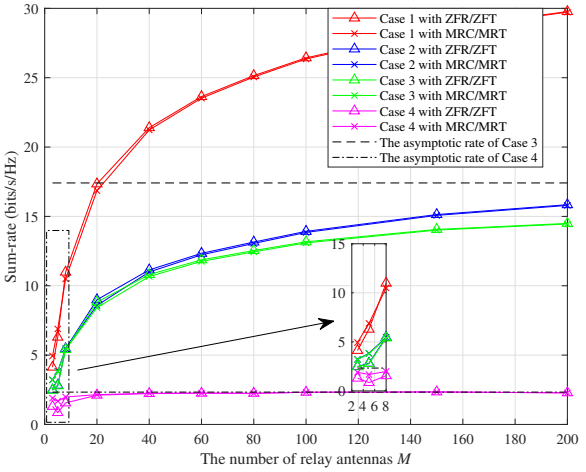

(b) $\vartheta = 1$.

Fig. 3: Achievable sum-rate versus the number of relay antennas M, $\sigma^2 = -50$ dBm.

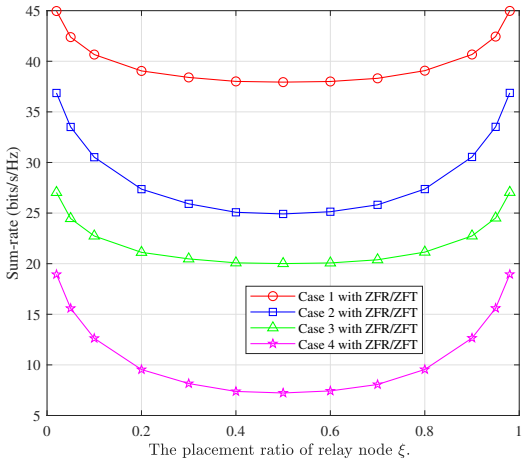

Fig. 4: Achievable sum-rate versus the placement ratio of relay node, $\vartheta = 3$, $\sigma^2 = -50$ dBm, $M = 500$.

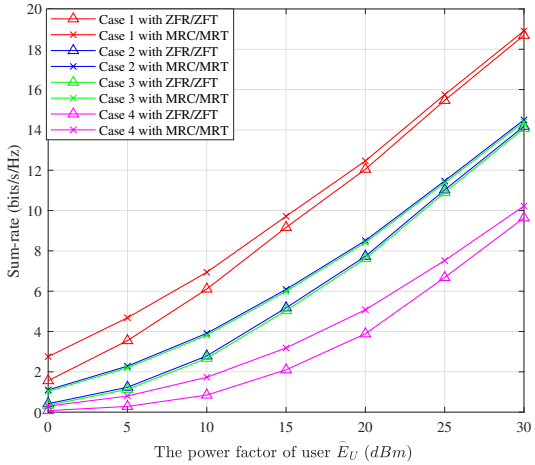

(a) $M = 5$.

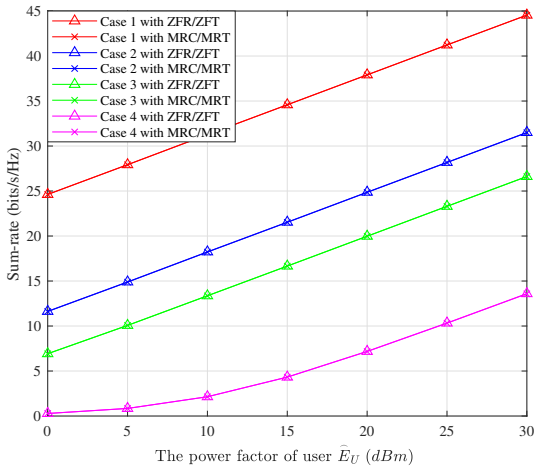

(b) $M = 500$.

Fig. 5: Achievable sum-rate versus the power factor of user $\widehat{E}_U$, $\vartheta = 3$, $\sigma^2 = -40$ dBm.

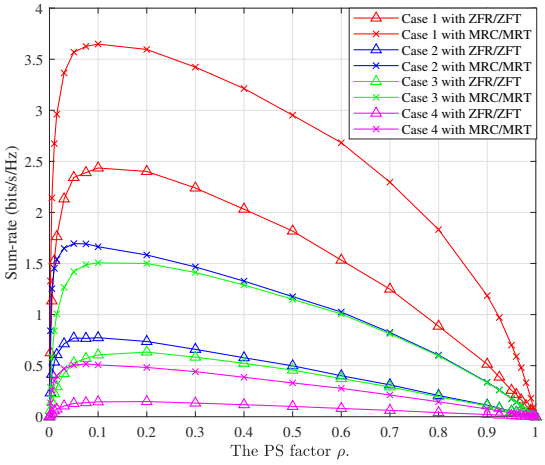

(a) $M = 5$.

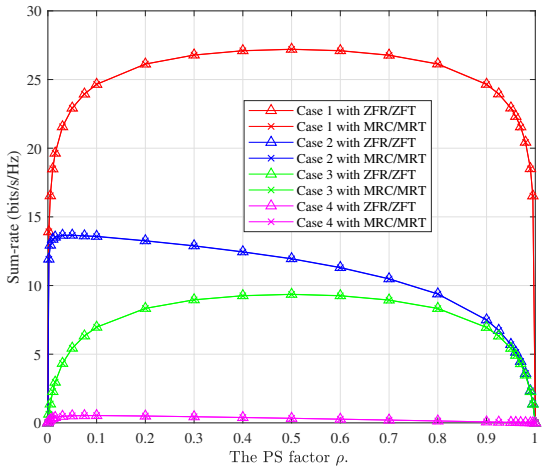

(b) $M = 500$.

Fig. 6: Achievable sum-rate versus the PS factor ρ, $\vartheta = 1$, $\sigma^2 = -40$ dBm.

almost the same rate performance. This can be obtained by the fact that when M grows large, the orthogonal channels are easy to be obtained for two precodings and the sum-rates are derived based on the assumption that the self-interference can be cancelled perfectly at two users.

Fig. 4 demonstrates the effect of the placement ratio of relay node on the sum-rates performance of massive MIMO relay system. It is intuitive that when ξ is small, the sum-rates of four cases decrease as ξ increases. Nonetheless, when ξ is large, the rate performance will improve as ξ grows. One reason is that the closer R is located to U_1 or U_2, the more EH efficiency R has. Besides, when R is close to U_i, the MIMO channel between R and U_i has better channel quality.

Fig. 5 reveals the influence of the user power factor on the sum-rate performance. Obviously, the achievable sum-rates of four power scaling cases grow unboundedly as $\widehat{E}_U$ increases. However, when $M = 5$, the sum-rates increase non-linearly with $\widehat{E}_U$ and the rate performance with MRC/MRT relay precoding is better that with ZFR/ZFT relay precoding that is

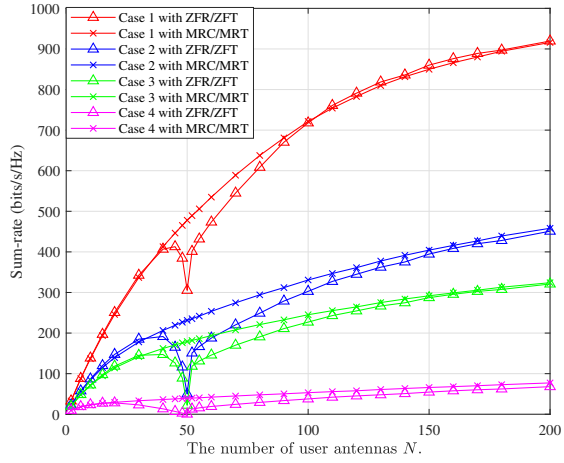

Fig. 7: Achievable sum-rate versus the number of user antennas, $\vartheta = 3$, $\sigma^2 = -50$ dBm, $M = 100$.

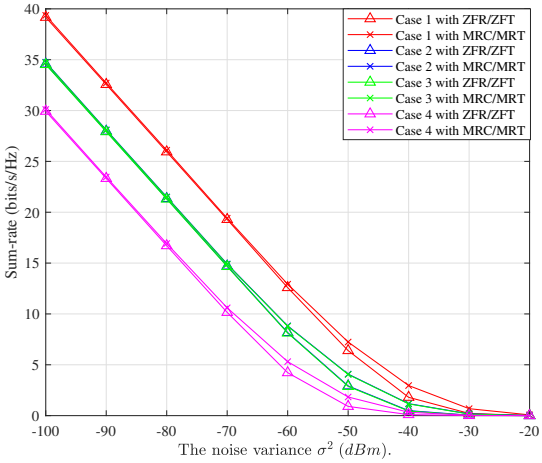

(a) $M = 5$.

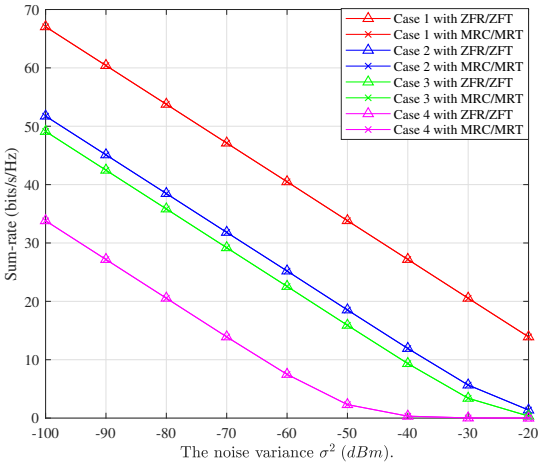

(b) $M = 500$.

Fig. 8: Achievable sum-rate versus the noise variance σ^2, $\vartheta = 1$.

consistent with the simulation results of Fig. 3 . When M is equal to 500, the sum-rates of Case 1 and 2 grow linearly with increasing $\widehat{E}_U$. Besides, it is intuitive that two relay precoding schemes, i.e,, MRC/MRT and the ZFR/ZFT, have almost the same rate performance when $M = 500$.

Fig. 6 describes the achievable sum-rate versus the PS factor of relay node. It can be noticed that the sum-rates of four power scaling cases are concave function with the PS factor of relay node. Similar to the results of Fig. 3, when $M = 5$, the MRC/MRT precoding outperforms ZFR/ZFT precoding in whole region of ρ, while the gap between two precodings almost disappears when $M = 500$.

Fig. 7 illustrates the achievable rate versus the number of user antennas. It is seen that the sum-rates of all cases increase non-linearly with the growth of N. It is noteworthy that when the number of user antennas is equal to 50, i.e., $N = 50$, the sum-rates of four cases with ZFR/ZFT precoding is quite low. This is because for ZFR/ZFT relay precoding, when $2N = M$, the MIMO relay channels are very ill-conditioned to force

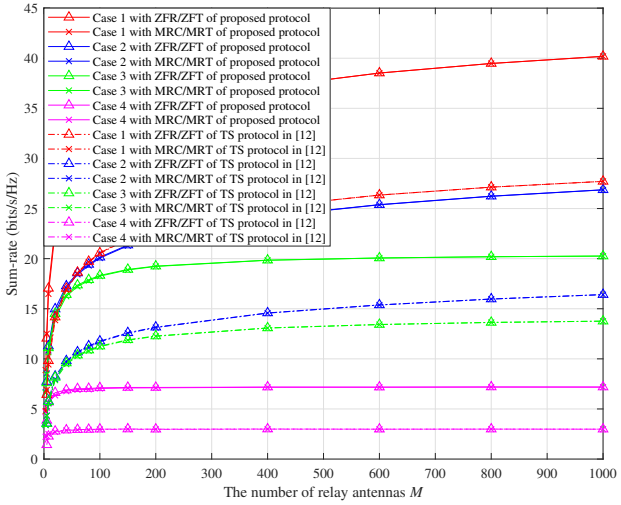

Fig. 9: Performance comparison between the proposed PS protocol and TS protocol, $\vartheta = 3$, $\sigma^2 = -50$ dBm.

inter-interference and noise to zero. Hence, it is hard to avoid the effect of noise enhancement. This is consistent with the result in [36].

Fig. 8 shows the impact of the noise variance σ^2 on the achievable sum-rate of massive MIMO relay system. It can be observed that the increase of σ^2 can decrease the achievable sum-rates of all cases. This is because the received SNRs at users become lower when σ^2 is larger. Interestingly, when σ^2 is large and $M = 5$, the relay system with MRC/MRT precoding has a better rate performance than that with ZFR/ZFT precoding, while the impact of the precoding scheme on the achievable sum-rate becomes smaller when M increases. There are two reasons accountable for this phenomenon. 1) Based on the above theoretical analysis, the achievable sum-rate is determined by the received SNRs at two users. When σ^2 is large and $M = 5$, the SNRs are low, which leads that the relay system with MRC/MRT precoding has the advantage over that with ZFR/ZFT precoding. 2) when $M = 500$, the channels created by ZFR/ZFT precoding become nearly orthogonal, which is consistent with the results of Fig. 3.

Fig. 9 compares the sum rate performance of the proposed PS relay protocol and the TS relay protocol in [12]. It is intuitive that the proposed PS relay protocol has a significant performance gain over the TS relay protocol in [12]. This is because compared to TS protocol, the PS protocol takes advantage of the broadcast character of RF signal to achieve the energy-rate trade-offs. This is consistent with the analysis and results in [37]. Besides, the TS two-way relay protocol of [12] abandons one-user energy gain in the EH phase, which leads that the relay node has less transmission power in the BC phase. Although the PS-based relay system has a better rate performance than the TS-based one, the practical circuit for TS protocol has a low complexity. According to the practical requirement, the relay systems are designed to achieve different tradeoffs between the performance and the complexity.

VII. Conclusion

In this paper, a massive MIMO two-way relaying system with ZFR/ZFT and MRC/MRT relay precodings has been studied in order to analyze and improve the performance of IoT networks. The SWIPT technique has been considered in the relay system to enhance the reliability. After deriving the deterministic sum-rate, the asymptotic performance of four classical power scaling cases has been studied and proved by the simulation results when the number of relay antennas increased to infinity. It was shown that the sum-rates of Case 3 and 4 converge to the corresponding asymptotic values. Besides, the PS factor and the placement ratio of relay node have a huge influence on the achievable sum-rates. Meanwhile, the impacts of the user power factor and the number of user antennas on the achievable rate were also discovered. These theoretical performance analyses will be significant for the practical application of massive MIMO relaying system. In future work, we will focus on the precoding and PS optimization for maximizing the sum-rate of MIMO two-way relaying system with SWIPT.

VIII. Acknowledgment

The authors sincerely thank the editor and anonymous reviewers for their helpful reviews and constructive comments, which have significantly improve the quality of the paper.

Appendix A
Proof of Proposition 2

Substituting (8) back into (5), we have

$$\frac{\mathbf{y}_i}{M} = \sqrt{\frac{E_U}{N}}\sqrt{\rho}\frac{\beta_{zf}}{M}\mathbf{G}_i\bar{\mathbf{F}}_{zf}\mathbf{H}_{\bar{i}}\mathbf{x}_{\bar{i}} + \sqrt{\rho}\frac{\beta_{zf}}{M}\mathbf{G}_i\bar{\mathbf{F}}_{zf}\mathbf{n}_R + \frac{\beta_{zf}}{M}\mathbf{G}_i\bar{\mathbf{F}}_{zf}\mathbf{n}_{R,\,z} + \frac{\mathbf{n}_i}{M}, \quad (60)$$

with $P_R = \widehat{E}_{RC}M$ and (22), we have

$$\frac{\beta_{zf}}{M} \xrightarrow[M\to\infty]{a.s.} \sqrt{\frac{\widehat{E}_{RC}L_1L_2\varphi_{ru_1}^2\varphi_{ru_2}^2}{\widehat{E}_U\rho\left(L_1\varphi_{ru_1}^2 + L_2\varphi_{ru_2}^2\right)}}. \quad (61)$$

Besides, on the basis of (26) and (32), we achieve the deterministic result as follows

$$\mathbf{G}_i\bar{\mathbf{F}}_{zf}\mathbf{H}_{\bar{i}} \xrightarrow[M\to\infty]{a.s.} \mathbf{T}_i, \quad \mathbf{G}_i\bar{\mathbf{F}}_{zf} \xrightarrow[M\to\infty]{a.s.} \mathbf{0}_{N\times M}, \quad (62)$$

Moreover, the noise term in (60) is limited by

$$\frac{\mathbf{n}_i}{M} \xrightarrow[M\to\infty]{a.s.} \mathbf{0}_{N\times N}. \quad (63)$$

Therefore, putting (61), (62) and (63) back into (60), the received signal in (46) can be achieved.

Appendix B
Proof of Proposition 3

Plugging the power scaling of Case 2 and (8) into (5), the received signal at U_i can be rewritten as

$$\frac{\mathbf{y}_i}{\sqrt{M}} = \sqrt{\frac{E_U}{N}}\sqrt{\rho}\frac{\beta_{zf}}{\sqrt{M}}\mathbf{G}_i\bar{\mathbf{F}}_{zf}\mathbf{H}_{\bar{i}}\mathbf{x}_{\bar{i}} + \sqrt{\rho}\frac{\beta_{zf}}{\sqrt{M}}\mathbf{G}_i\bar{\mathbf{F}}_{zf}\mathbf{n}_R + \frac{\beta_{zf}}{\sqrt{M}}\mathbf{G}_i\bar{\mathbf{F}}_{zf}\mathbf{n}_{R,\,z} + \frac{\mathbf{n}_i}{\sqrt{M}}. \quad (64)$$

Similar to (61), with $P_R \xrightarrow[M\to\infty]{a.s.} \widehat{E}_{RC}$, we achieve

$$\frac{\beta_{zf}}{\sqrt{M}} \xrightarrow[M\to\infty]{a.s.} \sqrt{\frac{\widehat{E}_{RC}L_1L_2\varphi_{ru_1}^2\varphi_{ru_2}^2}{\widehat{E}_U\rho\left(L_1\varphi_{ru_1}^2 + L_2\varphi_{ru_2}^2\right)}}. \quad (65)$$

Therefore, substituting (62), (63)and (65) back into (64), we can obtain (47). This completes the proof.

Appendix C
Proof of Proposition 4

Putting (35) into (5), we have

$$\frac{\mathbf{y}_i}{M} = \sqrt{\frac{E_U}{N}}\sqrt{\rho}M\beta_{mr}\frac{\mathbf{G}_i\bar{\mathbf{F}}_{mr}\mathbf{H}_{\bar{i}}}{M^2}\mathbf{x}_{\bar{i}} + \sqrt{\rho}M\beta_{mr}\frac{\mathbf{G}_i\bar{\mathbf{F}}_{mr}}{M^2}\mathbf{n}_R + M\beta_{mr}\frac{\mathbf{G}_i\bar{\mathbf{F}}_{mr}}{M^2}\mathbf{n}_{R,\,z} + \frac{\mathbf{n}_i}{M}. \quad (66)$$

With $P_R = \widehat{E}_{RC}M$, (34) and (41), we achieve

$$M\beta_{mr} \xrightarrow[M\to\infty]{a.s.} \sqrt{\frac{\widehat{E}_{RC}}{\widehat{E}_U\rho\left(\sum_{i=1}^{2}L_{\bar{i}}L_i^2\varphi_{ru_{\bar{i}}}^2\varphi_{u_ir}^4\right)}}. \quad (67)$$

Substituting the definition of $\bar{\mathbf{F}}_{mr}$ into the term $\frac{\mathbf{G}_i\bar{\mathbf{F}}_{mr}\mathbf{H}_{\bar{i}}}{M^2}$, we have

$$\frac{\mathbf{G}_i\bar{\mathbf{F}}_{mr}\mathbf{H}_{\bar{i}}}{M^2} = \sum_{j=1}^{2}\frac{\mathbf{G}_i\mathbf{G}_{\bar{j}}^H}{M}\mathbf{T}_{\bar{j}}\frac{\mathbf{H}_{\bar{j}}^H\mathbf{H}_{\bar{i}}}{M} \xrightarrow[M\to\infty]{a.s.} L_iL_{\bar{i}}\varphi_{ru_i}^2\varphi_{u_{\bar{i}}r}^2\mathbf{T}_i. \quad (68)$$

Besides, we have

$$\frac{\mathbf{G}_i\bar{\mathbf{F}}_{mr}}{M^2} \xrightarrow[M\to\infty]{a.s.} \mathbf{0}_{N\times M}, \quad \frac{\mathbf{n}_i}{M} \xrightarrow[M\to\infty]{a.s.} \mathbf{0}_{N\times 1} \quad (69)$$

Finally, Substituting (67), (68) and (69) back into (66), (53) is obtained for Case 1 when $M\to\infty$.

Appendix D
Proof of Proposition 5

Substituting the power scaling of Case 2 and (35) into (5), the received signal at U_i can be re-expressed by

$$\frac{\mathbf{y}_i}{\sqrt{M}} = \sqrt{\frac{E_U}{N}}\sqrt{\rho}M^{\frac{3}{2}}\beta_{mr}\frac{\mathbf{G}_i\bar{\mathbf{F}}_{mr}\mathbf{H}_{\bar{i}}}{M^2}\mathbf{x}_{\bar{i}} + \sqrt{\rho}M^{\frac{3}{2}}\beta_{mr}\frac{\mathbf{G}_i\bar{\mathbf{F}}_{mr}}{M^2}\mathbf{n}_R + M^{\frac{3}{2}}\beta_{mr}\frac{\mathbf{G}_i\bar{\mathbf{F}}_{mr}}{M^2}\mathbf{n}_{R,\,z} + \frac{\mathbf{n}_i}{M} \quad (70)$$

Similar to (67), with $P_R \xrightarrow[M\to\infty]{a.s.} \widehat{E}_{RC}$, we obtain

$$M^{\frac{3}{2}}\beta_{mr} \xrightarrow[M\to\infty]{a.s.} \sqrt{\frac{\widehat{E}_{RC}}{\widehat{E}_U \rho \left(\sum_{i=1}^{2} L_{\bar{i}} L_i^2 \varphi_{ru_{\bar{i}}}^2 \varphi_{u_i r}^4 \right)}}. \quad (71)$$

Therefore, putting (68), (69) and (70) into (71), we can achieve (54). This completes the proof.

REFERENCES

[1] N. Zhao et al., "UAV-Assisted Emergency Networks in Disasters," *IEEE Wireless Commun.*, vol. 26, no. 1, pp. 45-51, Feb. 2019.

[2] S. Hu et al., "Non-orthogonal Interleave-Grid Multiple Access Scheme for Industrial Internet-of-things in 5G Network," *IEEE Trans. Ind. Informatics*, vol. 14, no. 12, pp. 5436-5446, Dec. 2018.

[3] Q. Qi, X. Chen and D. W. K. Ng, "Robust Beamforming for NOMA-Based Cellular Massive IoT With SWIPT," *IEEE Trans. Signal Process.*, vol. 68, pp. 211-224, 2020.

[4] X. Liu, M. Jia, X. Zhang and W. Lu, "A Novel Multichannel Internet of Things Based on Dynamic Spectrum Sharing in 5G Communication," *IEEE Internet Things J.*, vol. 6, no. 4, pp. 5962-5970, Aug. 2019.

[5] W. Lu, S. Hu, X. Liu, C. He, Y. Gong, "Incentive Mechanism Based Cooperative Spectrum Sharing for OFDM Cognitive IoT Network", *IEEE Trans. Netw. Sci. Eng.*, May 2019.

[6] X. Liu and X. Zhang, "NOMA-Based Resource Allocation for Cluster-Based Cognitive Industrial Internet of Things," *IEEE Trans. Ind. Informatics*, vol. 16, no. 8, pp. 5379-5388, Aug. 2020.

[7] D. Zhai, H. Chen, Z. Lin, Y. Li and B. Vucetic, "Accumulate Then Transmit: Multiuser Scheduling in Full-Duplex Wireless-Powered IoT Systems," *IEEE Internet Things J.*, vol. 5, no. 4, pp. 2753-2767, Aug. 2018.

[8] Y. Ma, H. Chen, Z. Lin, Y. Li and B. Vucetic, "Distributed and Optimal Resource Allocation for Power Beacon-Assisted Wireless-Powered Communications," *IEEE Trans. Commun.*, vol. 63, no. 10, pp. 3569-3583, Oct. 2015.

[9] Z. Ding et al., "Application of smart antenna technologies in simultaneous wireless information and power transfer," *IEEE Commun. Mag.*, vol. 53, no. 4, pp. 86-93, Apr. 2015.

[10] M. Alageli, A. Ikhlef and J. Chambers, "SWIPT Massive MIMO Systems With Active Eavesdropping," *IEEE J. Sel. Areas Commun.*, vol. 37, no. 1, pp. 233-247, Jan. 2019.

[11] R. Zhang and C. K. Ho, "MIMO Broadcasting for Simultaneous Wireless Information and Power Transfer," *IEEE Trans. Wireless Commun.*, vol. 12, no. 5, pp. 1989-2001, May 2013.

[12] S. Modem and S. Prakriya, "Optimization of Two-Way Relaying Networks With Battery-Assisted EH Relays," *IEEE Trans. Commun.*, vol. 66, no. 10, pp. 4414-4430, Oct. 2018.

[13] Y. Ye, L. Shi, X. Chu, H. Zhang and G. Lu, "On the Outage Performance of SWIPT-Based Three-Step Two-Way DF Relay Networks," *IEEE Trans. Veh. Technol.*, vol. 68, no. 3, pp. 3016-3021, Mar. 2019.

[14] R. Zhang, B. Shim and H. Zhao, "Downlink Compressive Channel Estimation with Phase Noise in Massive MIMO Systems," *IEEE Trans. Commun.*, Early access, doi: 10.1109/TCOMM.2020.2998141.

[15] Liu D L, Wu F, Quan X, et al. "Energy and spectral-efficiency of zero-forcing beamforming in massive MIMO systems with imperfect reciprocity calibration: bound and optimization. *Sci China Inf Sci*, 2018, 61(12): 122302, https://doi.org/10.1007/s11432-018-9591-8.

[16] Wu Z K, Fei Z S. "Precoder design in downlink CoMP-JT MIMO network via WMMSE and asynchronous ADMM. *Sci China Inf Sci*, 2018, 61(8): 082306, https://doi.org/10.1007/s11432-017-9275-y.

[17] J. Tang, D. K. C. So, N. Zhao, A. Shojaeifard and K. Wong, "Energy Efficiency Optimization With SWIPT in MIMO Broadcast Channels for Internet of Things," *IEEE Internet Things J.*, vol. 5, no. 4, pp. 2605-2619, Aug. 2018.

[18] Y. Hu, Y. Zhu, M. C. Gursoy and A. Schmeink, "SWIPT-Enabled Relaying in IoT Networks Operating With Finite Blocklength Codes," *IEEE J. Sel. Areas Commun.*, vol. 37, no. 1, pp. 74-88, Jan. 2019.

[19] M. Alageli, A. Ikhlef and J. Chambers, "Optimization for Maximizing Sum Secrecy Rate in MU-MISO SWIPT Systems," *IEEE Trans. Veh. Technol.*, vol. 67, no. 1, pp. 537-553, Jan. 2018.

[20] Z. Zhang, Z. Chen, M. Shen and B. Xia, "Spectral and Energy Efficiency of Multipair Two-Way Full-Duplex Relay Systems With Massive MIMO," *IEEE J. Sel. Areas Commun.*, vol. 34, no. 4, pp. 848-863, Apr. 2016.

[21] J. Feng, S. Ma, G. Yang and H. V. Poor, "Impact of Antenna Correlation on Full-Duplex Two-Way Massive MIMO Relaying Systems," *IEEE Trans. Wireless Commun.*, vol. 17, no. 6, pp. 3572-3587, Jun. 2018.

[22] J. Feng, S. Ma, G. Yang and B. Xia, "Power Scaling of Full-Duplex Two-Way Massive MIMO Relay Systems With Correlated Antennas and MRC/MRT Processing," *IEEE Trans. Wireless Commun.*, vol. 16, no. 7, pp. 4738-4753, July 2017.

[23] Z. Wen, W. Guo, N. C. Beaulieu, X. Liu and W. Xu, "Performance of SWIPT for AF MIMO Relay Systems With Direct Link," *IEEE Commun. Lett.*, vol. 22, no. 2, pp. 340-343, Feb. 2018.

[24] T. A. Khan, A. Yazdan, and R. W. Heath, "Optimization of power transfer efficiency and energy efficiency for wireless-powered systems with massive MIMO,"*IEEE Trans. Wireless Commun.*, vol. 17, no. 11, pp. 7159-7172, Nov. 2018.

[25] J. Wang, G. Wang, Z. Lin, L. Zheng and M. Ding, "SWIPT in MIMO AF Relay Systems with Direct Link," in *Proc. IEEE 89th Veh. Technol. Conf. (VTC Spring)*, Apr. 2019, pp. 1-6.

[26] B. Li and Y. Rong, "Joint Transceiver Optimization for Wireless Information and Energy Transfer in Nonregenerative MIMO Relay Systems," *IEEE Trans. Veh. Technol.*, vol. 67, no. 9, pp. 8348-8362, Sep. 2018.

[27] J. Feng, S. Ma, G. Yang and B. Xia, "Wireless Information and Power Transfer in Full-Duplex Two-Way Massive MIMO AF Relay Systems," in *Proc. IEEE 85th Veh. Technol. Conf. (VTC Spring)*, Jun. 2017, pp. 1-5.

[28] J. Wang, G. Wang, H. Yang, B. Li and T. Zhang, "Joint Transceiver Optimization for Multiuser Multi-Antenna Relay Systems With Energy Harvesting," *IEEE Access*, vol. 7, pp. 151156-151167, 2019.

[29] Z. Wen, X. Liu, S. Zheng, and W. Guo, "Joint source and relay design for MIMO two-way relay networks with SWIPT," *IEEE Trans. Veh. Technol.*, vol. 67, no. 1, pp. 822-826, Jan. 2018.

[30] W. Wang, R. Wang, H. Mehrpouyan, N. Zhao and G. Zhang, "Beamforming for Simultaneous Wireless Information and Power Transfer in Two-Way Relay Channels," *IEEE Access*, vol. 5, pp. 9235-9250, 2017.

[31] J. Wang, L. Zheng, M. Ding, G. Wang and Z. Lin, "Performance Analysis of Massive MIMO Two-Way Relay Systems with SWIPT," in *Proc. IEEE 89th Veh. Technol. Conf. (VTC Spring)*, Apr. 2019, pp. 1-6.

[32] J. Rostampoor, S. M. Razavizadeh and I. Lee, "Energy Efficient Precoding Design for SWIPT in MIMO Two-Way Relay Networks," *IEEE Trans. Veh. Technol.*, vol. 66, no. 9, pp. 7888-7896, Sep. 2017.

[33] T. Koch, "Is the assumption of perfect channel-state information in fading channels a good assumption? " in *Proc. 2nd Int. Symp. Appl. Sci. Biomed. Commun. Technol.*, Nov. 2009, pp. 1-6.

[34] A. Pastore, T. Koch, and J. R. Fonollosa, "A rate-splitting approach to fading channels with imperfect channel-state information," *IEEE Trans. Inf. Theory*, vol. 60, no. 7, pp. 4266–4285, Jul. 2014.

[35] R. Wang and M. Tao, "Joint source and relay precoding designs for MIMO two-way relaying based on MSE criterion," *IEEE Trans. Signal Process.*, vol. 60, no. 3, pp. 1352–1365, Mar. 2012.

[36] Y. Zhang, L. Ping and Z. Zhang, "Low Cost Pre-Coder Design for MIMO AF Two-Way Relay Channel," *IEEE Signal Process. Lett.*, vol. 22, no. 9, pp. 1369-1372, Sept. 2015.

[37] X. Zhou, R. Zhang and C. K. Ho,"Wireless Information and Power Transfer: Architecture Design and Rate-Energy Tradeoff," *IEEE Trans. Commun.*, vol. 61, no. 11, pp. 4754-4767, Nov. 2013.

Jinlong Wang received the B.S. and M.S. degrees from Electronic Engineering College, Heilongjiang University, China, in 2010 and 2013, respectively. From December 2015 to December 2017, he was a Visiting Ph.D. student with the School of Electrical and Information Engineering, University of Sydney, Australia. He is currently pursuing the Ph.D. degree in communication engineering with the Harbin Institute of Technology, China. His research interests include MIMO relay system, wireless power transfer, and UAV communications.

Gang Wang (M'11) received the B.E., M.E., and Ph.D. degrees in communication engineering from the Harbin Institute of Technology, Harbin, China, in 1984, 1987, and 2007, respectively. He is currently a Professor with the Communication Research Center, Harbin Institute of Technology. He is also the Chairman of the Department of Communication Engineering. He has published over 60 research papers and 4 books. His general interests include ad hoc networks, wireless communications, and artificial intelligence. He was a recipient of the National Grade II Prize of Science and Technology Progress and the National Grade III Prize of Science and Technology Progress.

Bo Li (M'19) received the bachelor's degree in communication engineering and the master's degree and Ph.D. degrees in information and communication engineering from the Harbin Institute of Technology, China, in 2007, 2009, and 2013, respectively. He was a Visiting Ph.D. Student with the School of EEE, Nanyang Technological University, Singapore, from 2012 to 2013. Since 2013, he has been with the School of Information and Electrical Engineering, Harbin Institute of Technology, Weihai, China, as an associate professor. His interested research areas are physical layer network coding, mobile ad hoc networks, and adaptive modulation and coding.

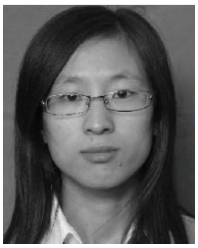

Hongjuan Yang (M'19) received the bachelor's degree in communication engineering from Jilin University, China, in 2007, and the master's and Ph.D. degrees in information and communication engineering from the Harbin Institute of Technology, China, in 2009 and 2013, respectively. She was a Visiting Ph.D. student with the School of EEE, Nanyang Technological University, Singapore, from 2012 to 2013. Since 2013, she has been a Lecturer with the School of Information and Electrical Engineering, Harbin Institute of Technology, Weihai, China. Her interested research areas are cooperative diversity technology, physical-layer network coding, and delay tolerant networks.

Yulin Hu (S'11-M'15-SM'18) received the M.Sc.E.E. degree from USTC, China, in 2011, and the Ph.D.E.E. degree (Hons.) from RWTH Aachen University. He completed the dissertation of the joint Ph.D. degree under the supervision of Prof. A. Schmeink with RWTH Aachen University, and under the supervision of Prof. J. Gross with the KTH Royal Institute of Technology in 2015 . He was a Research Fellow with RWTH Aachen University in 2016. In 2017, he was a Visiting Scholar with Prof. M. C. Gursoy in Syracuse University, USA. Since 2017, he has been a Senior Researcher and the Project Lead with the ISEK Research Group, RWTH Aachen University. His research interests are in information theory and optimal design of wireless communication systems. He has been invited to contribute submissions to multiple conferences. He was a recipient of the IFIP/IEEE Wireless Days Student Travel Awards in 2012. He received the Best Paper Awards from the IEEE ISWCS 2017 and the IEEE PIMRC 2017. He is currently serving as an Editor for the Physical Communication (Elsevier).

Anke Schmeink (M'11–SM'18) received the Diploma degree in mathematics in medicine and the Ph.D. degree in electrical engineering and information technology from RWTH Aachen University, Germany, in 2002 and 2006, respectively. She was a Research Scientist with Philips Research before joining RWTH Aachen University in 2008, where she has been an Associate Professor since 2012. She spent several research visits with The University of Melbourne and the University of York. She is a member of the Young Academy, North Rhine-Westphalia Academy of Sciences. Her research interests are in information theory, systematic design of communication systems, and bioinspired signal processing.